Small RNA-mediated chromatin silencing directed to the 3′ region of the *Arabidopsis* gene encoding the developmental regulator, FLC

Szymon Swiezewski*†, Pedro Crevillen*, Fuquan Liu*, Joseph R. Ecker‡, Andrzej Jerzmanowski†§, and Caroline Dean*¶

*Department of Cell and Developmental Biology, John Innes Centre, Norwich NR4 7UH, United Kingdom; †Institute of Biochemistry and Biophysics, Polish Academy of Sciences, 02-106 Warsaw, Poland; ‡The Salk Institute for Biological Studies, La Jolla, CA 92037; and §Laboratory of Plant Molecular Biology, Warsaw University, 02-106 Warsaw, Poland

Contributed by Joseph R. Ecker, December 22, 2006 (sent for review September 29, 2006)

Small RNA-mediated chromatin silencing is well characterized for repeated sequences and transposons, but its role in regulating single-copy endogenous genes is unclear. We have identified two small RNAs (30 and 24 nucleotides) corresponding to the reverse strand 3′ to the canonical poly(A) site of *FLOWERING LOCUS C* (*FLC*), an *Arabidopsis* gene encoding a repressor of flowering. Genome searches suggest that these RNAs originate from the *FLC* locus in a genomic region lacking repeats. The 24-nt small RNA, which is most abundant in developing fruits, is absent in mutants defective in RNA polymerase IVa, RNA-DEPENDENT RNA POLYMERASE 2, and DICER-LIKE 3, components required for RNAi-mediated chromatin silencing. The corresponding genomic region shows histone 3 lysine 9 dimethylation, which was reduced in a *dcl2,3,4* triple mutant. Investigations into the origins of the small RNAs revealed a polymerase IVa-dependent spliced, antisense transcript covering the 3′ *FLC* region. Mutation of this genomic region by T-DNA insertion led to *FLC* misexpression and delayed flowering, suggesting that RNAi-mediated chromatin modification is an important component of endogenous pathways that function to suppress *FLC* expression.

flowering | small interfering RNA | antisense transcription

The role of the RNAi machinery in the epigenetic silencing of repeated sequences and transposons is well documented (1). Double-stranded RNA, generated by a variety of mechanisms including antisense transcription, transcription through inverted repeats, or RDR activity, is cleaved by DICER(s) (DCL) to produce short interfering (si)RNAs, which direct chromatin-modifying machinery to regions of the chromatin containing complementary DNA sequences. The siRNAs and chromatin-modification complexes are tethered to the silenced loci, maintaining continued production of siRNAs and the silenced state.

In *Arabidopsis*, the production and function of siRNAs mediating the epigenetic silencing of repeated sequences require RDR2, DCL3, HUA ENHANCER 1 (HEN1), ARGONAUTE (AGO) 4 (2–4), and two functionally distinct forms of a plant-specific RNA polymerase IV complex, containing either polymerase IV largest subunit (NRPD) 1a or NRPD1b with NRPD2 (5–8). Several observations suggest that RNAi-mediated chromatin silencing could also be playing a major role in regulation of single-copy sequences. siRNAs complementary to both genic and intergenic sequences have been identified in *Arabidopsis* (9) and associated with AGO4 (10). In mammals, DICER has been shown to play a role in the turnover of intergenic transcripts and the corresponding chromatin modification in the human β-globin cluster (11), and antisense/intergenic transcripts have been found to be extensive in the *Arabidopsis*, *Drosophila*, and mammalian genomes (12, 13). Cis-antisense transcripts have also been shown to trigger posttranscriptional silencing, conferring salt tolerance and plant immunity in *Arabidopsis* (14, 15).

Considerable activity has focused on dissecting the epigenetic basis of the regulation of *FLC*, a MADS box transcription factor that represses the transition to flowering in *Arabidopsis* (16, 17). *FLC* expression is repressed by prolonged cold (experienced as the plants overwinter), and this repression is maintained epigenetically through the subsequent development of the plant. This process is known as vernalization, and an analysis of mutants defective in vernalization identified VERNALIZATION2 (VRN2), a Polycomb-group protein homologous to Su(Z)12 (18), VERNALIZATION1 (VRN1), a plant specific protein with DNA-binding domains (19), and VERNALIZATION-INDEPENDENT3 (VIN3), a PHD (plant homeodomain) protein (20) as regulators of the process. These proteins mediate the cold-induced histone deacetylation and methylation changes at *FLC*, required for the epigenetic silencing (20, 21). A role for the *Arabidopsis* HETEROCHROMATIN PROTEIN 1 (HP1) homolog, Like HP1 (LHP1), in the epigenetic silencing of *FLC* has also been found (22, 23).

FLC expression is also repressed by a series of proteins (FCA, FY, FLD, FVE, FPA, FLK, and LD) grouped into the autonomous pathway. The late flowering loss-of-function phenotype of these genes can be overcome by vernalization, suggesting that the vernalization and autonomous pathways function in parallel. The components of the autonomous pathway have all been cloned and are involved in RNA binding (FCA, FPA, and FLK), RNA processing (FY), or chromatin regulation (FVE, FLD). Our current understanding of their function has been reviewed recently (24).

As part of the dissection of *FLC* regulation, we have investigated the role of the RNAi machinery in *FLC* regulation and here describe the identification of 30- and 24-nucleotide small RNAs complementary to the *FLC* sense strand 3′ to the major poly(A) site. We have characterized their accumulation and demonstrated the presence of a corresponding antisense transcript whose levels were reduced in mutants defective in polymerase IVa. The corresponding genomic region of *FLC* was found to be enriched for histone 3 lysine 9 dimethylation (H3K9me2) in a DICER-dependent manner. Disruption of this *FLC* genomic region led to *FLC* misexpression and altered flowering time, demonstrating its functional importance in *FLC* regulation.

Results

Small RNA Homologous to *FLC* 3′ Region. Extensive Northern blot analysis was used to search for small RNAs homologous to *FLC*. Total RNA was isolated from a range of tissues, including inflorescences and seedlings of *Arabidopsis thaliana* accession

Author contributions: S.S., A.J., and C.D. designed research; S.S., P.C., and F.L. performed research; J.R.E. contributed new reagents/analytic tools; S.S. analyzed data; and S.S. and C.D. wrote the paper.

The authors declare no conflict of interest.

Abbreviations: DCL, DICER-LIKE; H3K9me2, histone 3 lysine 9 dimethylation.

¶To whom correspondence should be addressed. E-mail: caroline.dean@bbsrc.ac.uk.

This article contains supporting information online at www.pnas.org/cgi/content/full/0611459104/DC1.

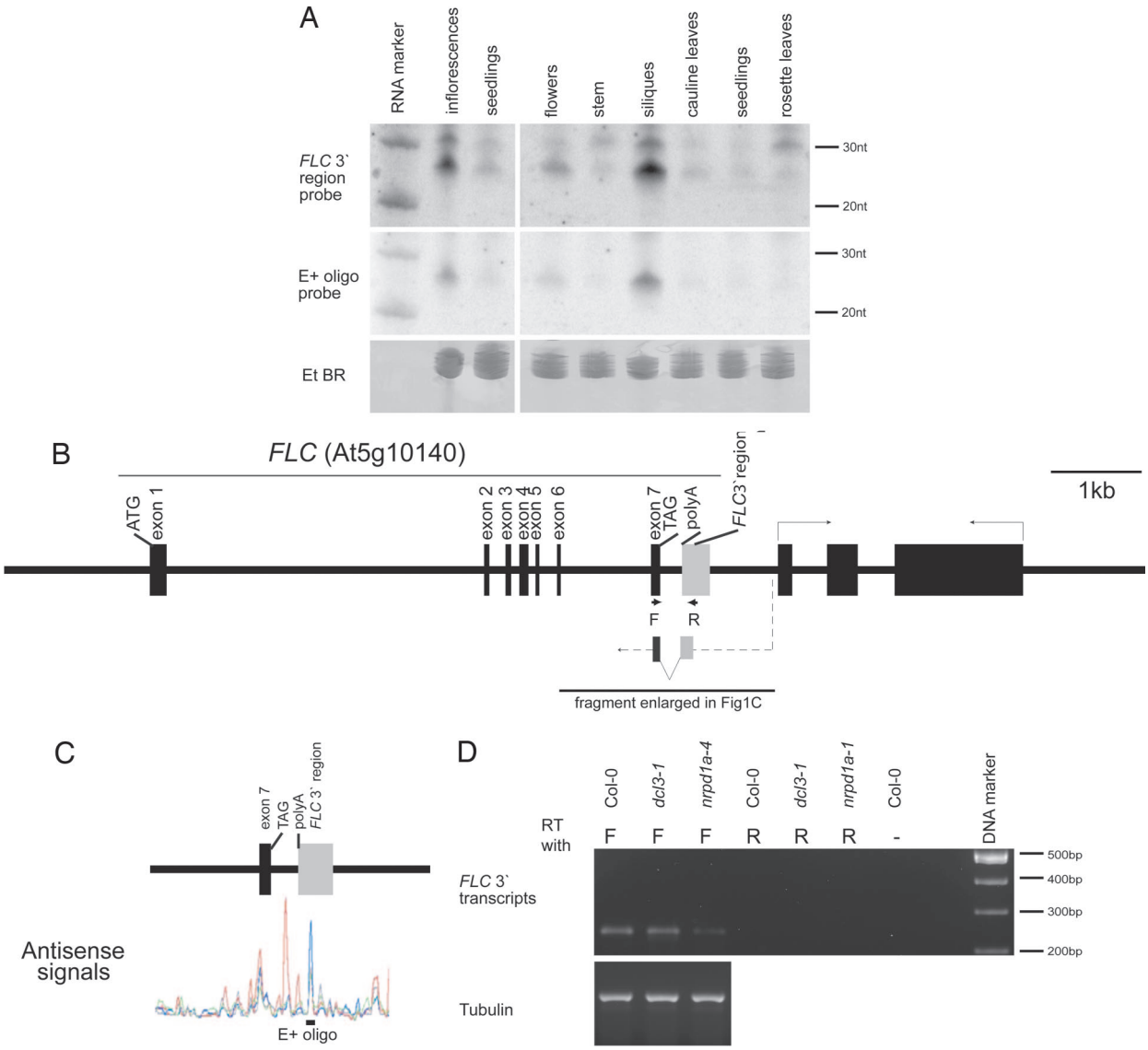

Fig. 1. Detection of small RNAs and antisense transcripts in *FLC* 3′ region. (*A*) Distribution of *FLC* 3′ small RNA in different organs and developmental stages of *Arabidopsis*. Total RNA isolated from different tissues of *Arabidopsis* was hybridized with either a 300-nt *FLC* 3′ fragment or an oligonucleotide (E+) that had shown strong hybridization in the whole-genome tiling arrays (12). The ethidium bromide staining is shown as a loading control. (*Left*) Prolonged exposure of a Northern blot carrying RNA isolated from seedlings and inflorescences. (*Right*) Northern blot hybridization to RNA isolated from different organs and stages of *Arabidopsis*. An RNA marker resolved on the same gel was used to size the *FLC* small RNA. (*B*) Schematic representation of the *FLC* locus with exons shown as thick black bars and introns represented by black lines joining the exons. The gray rectangle represents the *FLC* 3′ region described in the paper. A schematic representation of the antisense transcript and location of primers used to amplify it are also shown. (*C*) Representation of the data from ref. 12 of the antisense signals detected in 3′ region of *FLC*. Poly(A)$^+$ RNA had been extracted from different tissues: mixed-stage flowers (*blue*), seedlings (*red*), root (*green*), and cell culture (*black*). The location of the E+ oligonucleotide probe is shown. (*D*) Detection of an antisense transcript from the 3′ end of *FLC* by ssRT-PCR in seedlings of Col-0, *dcl3-1*, and *nrpd1a-4*.

Col-0 and hybridized with three *FLC* probes spanning the complete *FLC* locus. Small RNAs hybridizing to the 3′ end of *FLC* were detected in RNA from *A. thaliana* inflorescences (Fig. 1*A*). Subsequent use of smaller overlapping probes defined this hybridization to within a 300-nt fragment in the *FLC* 3′ region, marked on Fig. 1*B*. Oligonucleotide probes of 25 nts were designed from within this 300-nt interval, based on the sequences present on the *Arabidopsis* whole-genome tiling array (12), and they were used to probe the Northern blots. One oligonucleotide, 5′-agggacgtggctctctctctctctc-3′, corresponding to the sense *FLC* transcript, hybridized with a small RNA (marked E+ on Fig. 1 *A* and *C*). The oligonucleotide complementary to E+ did not show any hybridization, and the lack of detectable small RNAs homologous to the sense strand was subsequently confirmed by using longer RNA probes (data not shown). The E+ oligonucleotide appeared to account for the hybridization of the smaller of the two RNA species to the 300-nt fragment; however, we cannot exclude that other small RNA species of the same size hybridize to the 300-nt fragment.

The *FLC* 3′ small RNAs were sized against standard RNA markers and Cluster2 siRNA and found to be ≈30 and 24 nucleotides long [Fig. 1*A* and supporting information (SI) Fig. 5] (2). The four DCL proteins encoded in the *Arabidopsis* genome are thought to produce mainly 21-, 22-, or 24-nucleotide RNAs, although small RNAs of 28–33 nts have been found by using a cloning approach (25). The *FLC* 3′ small RNAs might

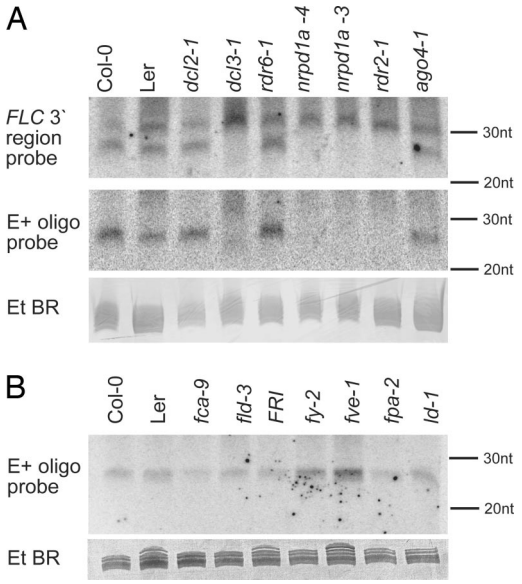

Fig. 2. *FLC* 3′ small RNA analysis in RNAi and autonomous pathway mutants. Total RNA was isolated from siliques of different *Arabidopsis* mutants impaired in RNAi pathways (as indicated above each lane) and hybridized with the E+ oligonucleotide. Ethidium bromide-stained gel is shown as a loading control.

also be modified posttranscriptionally (26). This *FLC* 3′ region shows no homology to other sequences, including transposons, as judged by analysis of the TIGR Plant Repeat Database and the RepeatMasker ASRP database. The sequence of the E+ oligonucleotide that hybridized to the 24-nt small RNA is unique in the *Arabidopsis* genome (FASTA search; best score, two mismatches).

The Small RNA Is Present in Seedlings and Developing Siliques. From the *Arabidopsis* whole genome tiling array analysis (12), an antisense signal had been detected corresponding to the region hybridizing to the small RNA, and it appeared most abundant in mixed-stage flowers (Fig. 1*C*). To investigate further the tissue specificity of the *FLC* small RNA, its abundance was analyzed in open flowers, stems, developing siliques (>8 mm), cauline leaves, young seedlings (with ≈4 leaves), and rosette leaves from mature plants. The *FLC* 3′ small RNA was detected in all tissues tested; however, the strongest hybridization signal in the Northern blot analysis was found in developing siliques (Fig. 1*A*), possibly indicating a high level of expression in embryos.

RNAi Chromatin Silencing Machinery Is Required for Production of the 24-Nucleotide *FLC* Small RNA. Analysis of different *dcl* mutants revealed that DCL3, the DICER associated with heterochromatic silencing, is required for the production of the 24-nt *FLC* 3′ small RNA (Fig. 2*A*). Consistent with this finding, it was also absent from two other mutants, *rdr2-1*, a mutation of an RNA-dependent RNA polymerase previously associated with heterochromatic silencing, and *nrpd1a*, a mutation in one of the large subunits of RNA polymerase IV. To date, all tested *rdr2*/*nrpd1a*/*dcl3*-dependent siRNAs have been implicated in chromatin silencing. The *FLC* 24-nt RNA accumulated normally in an *ago4* mutant, putting it into a group along with siRNA02 and Cluster2 siRNA (2, 27). Interestingly, the 30-nt small RNA species, whose production is not abolished in any of the tested mutants, was found to be consistently up-regulated in *dcl3-1* (Fig. 2*A*). In addition, smaller RNAs hybridized to both the 300-nt fragment and E+ in *dcl3-1* that were not present in wild-type Columbia (Fig. 2*A*).

The hybridization of the detectable *FLC* small RNAs to sequences just downstream of the major polyadenylation site of *FLC* suggested possible roles in defining the 3′ end of the transcript. FCA and FY, components of the autonomous pathway that repress *FLC* expression, function to regulate polyadenylation site choice, at least in the *FCA* transcript. Accumulation of the 24-nt *FLC* 3′ small RNA was therefore analyzed in autonomous pathway mutants *fca-9*, *fld-3*, *fy-2*, *fve-1*, *fpa-2*, and *ld-1* and in a genotype carrying an active *FRIGIDA* allele (which would up-regulate *FLC* steady-state mRNA levels). The small RNA was present in both the Landsberg *erecta* and Columbia *Arabidopsis* accessions, and its expression was not affected in any of the mutants tested (Fig. 2*B*).

Antisense Transcripts Corresponding to the Small RNA Region. To understand the origin of the small RNA, we investigated the nature of the antisense RNA transcripts predicted from the *Arabidopsis* whole-genome tiling array analysis (12). Using strand-specific RT-PCR, a weakly expressed antisense transcript could be detected in the *FLC* 3′ region (Fig. 1*D*). The amplified band was isolated and sequenced, revealing a transcript with a 222-nt intron. The predicted splicing junction is 5′-CACGAATAAG∧TAGTGGGAGA-3′. The intron is not present in any of the cloned sense transcripts originating from the region (as checked against the GenBank EST and full-length cDNA databases). Northern blots with single-stranded DNA probes confirmed the presence of this transcript and sized it as ≈700 nt long (data not shown). These results suggest the presence of a cryptic promoter in the *FLC* 3′ region priming antisense transcription that extends into the *FLC* coding sequence (at least into the last exon) as shown on Fig. 1*B*. The level of antisense transcript was not affected in *dcl3-1* but accumulated to a lower level in *nrpd1a-4*, suggesting that it may be the precursor to the small RNAs and a direct or indirect role for polymerase IVa in its production (Fig. 1*D*).

Role of FLC 3′ Small RNA in *FLC* Regulation. To test the functional significance of the *FLC* 3′ small RNA, *FLC* expression was analyzed in mutants defective in small RNA production (Fig. 3*A*). *dcl3-1*, *rdr2-1*, and *nrpd1a-3*,*-4*, all defective in *FLC* small RNA production, showed an up-regulation of *FLC* mRNA. The *dcl2-1* mutant, which did not abolish *FLC* 3′ small RNA production, did not show any change in *FLC* mRNA level. To investigate *FLC* 3′ small RNA function in *FLC* regulation more directly, we analyzed lines carrying T-DNA insertions in this region. Three SALK T-DNA insertion lines were selected, and the T-DNA insertion sites were mapped by PCR (Fig. 3*B*). Only the line with a T-DNA insertion located actually within the *FLC* 3′ region (*flc_utr4*) flowered later than Col-0, whereas the two lines with T-DNA inserted either upstream or downstream from the *FLC* 3′ region (*flc_utr3* and *flc_utr5*; Fig. 3*B*) showed an early flowering phenotype (Fig. 3*C*). The flowering time of the mutants lines correlates well with *FLC* mRNA level. A moderate increase in *FLC* mRNA was seen in *flc_utr4*, whereas a reduction was observed in both *flc_utr3* and *flc_utr5* lines (Fig. 3*D*). *FLC* repression therefore appears to be perturbed in *flc_utr4*. The reduction in *FLC* mRNA in *flc_utr5* is likely to be the result of disruption of the *cis* sequences required for polyadenylation site recognition. Similarly, the early flowering phenotype and reduction in *FLC* mRNA in the *flc_utr3* mutant, where the T-DNA is 890 bp 3′ to the processed transcript end, could result from disruption of the correct chromatin structure. Alternatively, the T-DNA insertions may be eliciting a silencing mechanism that will tend to give an overall reduction in expression of adjacent sequences because of local spreading of silent chromatin.

In contrast to discrete hybridization to 30- and 24-nt RNAs an *FLC* 3′ 300-nt probe hybridized to a smear of RNAs in *flc_utr4*

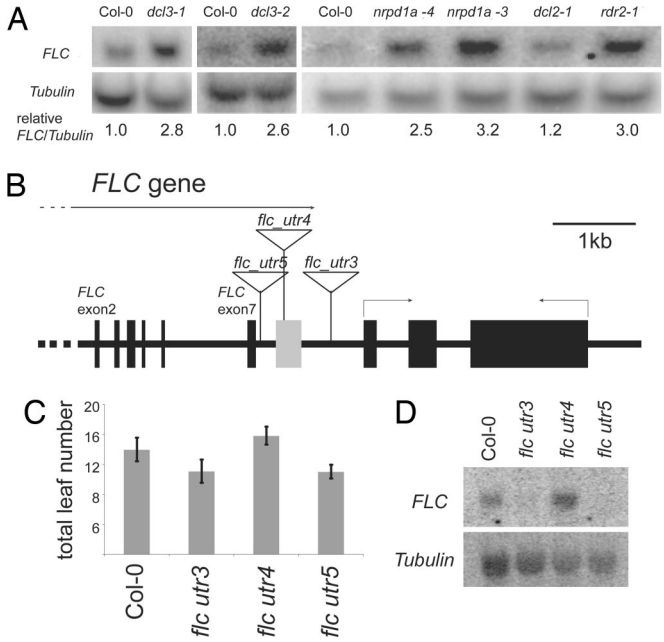

Fig. 3. *FLC* 3′ small RNAs are functionally important for *FLC* regulation. (*A*) Northern blot analysis of *FLC* mRNA levels in seedlings of Col-0, *dcl2-1*, *dcl3-1*, *nrpd1a-3*,*-4*, and *rdr2-1*. The blot was stripped and rehybridized with β-*TUBULIN* to monitor loading. (*B*) *FLC* locus annotated as in Fig. 1 with the location of three independent Salk T-DNA insertions mapped by PCR to different regions of *FLC*. (*C*) Flowering time data for Col-0, *flc_utr3*, *flc_utr4*, and *flc_utr5*. (*D*) Northern blot analysis of *FLC* mRNA levels in seedlings of Col-0, *flc_utr3*, *flc_utr4*, and *flc_utr5*. The blot was stripped and rehybridized with β-*TUBULIN*.

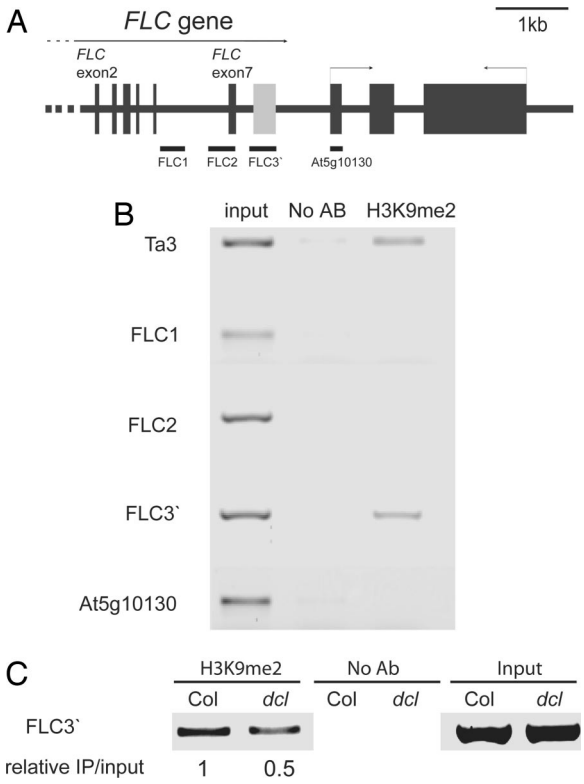

Fig. 4. Enrichment of H3K9me2 in the 3′ region of *FLC*. (*A*) Schematic representation of *FLC* and the downstream gene *At5g10130*. Exons are shown as thick black bars, and introns are represented by black lines joining the exons. The gray rectangle represents the *FLC* 3′ region described in the paper. Regions amplified by PCR are shown below as bars. (*B*) Semiquantitative PCR amplification of DNA immunoprecipitated by using an antibody specific for H3K9me2. Ta3 transposon amplification is shown as a positive control. Each ChIP was repeated twice, and the data shown are a representative picture. (*C*) ChIP analysis of H3K9me2 in the *FLC* 3′ region in Columbia (Col) and the triple *dcl2*, *3*, *4* mutant (*dcl*).

(data not shown), consistent with disruption of the production of the small RNAs by the T-DNA insertion. Lack of an *FLC* allele carrying a deletion of the 3′ region precludes a more definitive conclusion about their origin.

Histone Modifications Associated with Silent Chromatin Are Found in the 3′ Region of *FLC*. To gain insight into the possible mechanism of repression of *FLC* by the *FLC* 3′ small RNA, we analyzed the chromatin in the region and used chromatin immunoprecipitation (ChIP) experiments to assay levels of H3K9me2, a modification characteristic of repressed chromatin, in siliques and seedlings of Col-0 plants (Fig. 4 and data not shown). The *FLC* 3′ region was significantly and repeatedly enriched, compared with controls, after immunoprecipitation with an antibody to H3K9me2. The H3K9me2-enriched region was localized to the *FLC* 3′ region because DNA located 200 nt upstream and 750 nt downstream from this region was not significantly enriched in the immunoprecipitation.

The DCL3 dependence of the H3K9me2 was analyzed. A reduction in H3K9me2 levels was not detected in *dcl3-1* (data not shown) but was detected in a *dcl2*, *dcl3*, *dcl4* triple mutant (Fig. 4*C*). This observation suggests redundancy in function between different DICERs, consistent with the appearance of smaller hybridizing RNAs in the *dcl3* mutant (Fig. 2*A*).

Discussion

We have investigated whether RNAi-mediated chromatin silencing plays a role in the regulation of the single-copy *Arabidopsis* gene *FLC*, a central regulator in the control of flowering time. *FLC* is a target of multiple regulatory pathways that suppress its expression. The vernalization pathway involves cold-induced chromatin remodeling and epigenetic silencing (20, 21), and the autonomous pathway involves RNA processing and chromatin regulation (24, 28). Small RNAs corresponding to the reverse strand of *FLC* just 3′ to the major poly(A) site were detected. This region lacks any known transposon elements and does not share close homology with any other region in the *Arabidopsis* genome. The 24-nt small RNA was absent from mutants defective in RNAi chromatin silencing but not in mutants of the autonomous pathway. An antisense RNA was found that covered this region, and this RNA contained an intron not present in the sense strand, suggesting that it originated from antisense transcription. The next annotated gene in the genome 3′ to *FLC* is transcribed in the same orientation as *FLC* 1,430 bp downstream, so the antisense transcript is unlikely to originate from transcription from this gene. Mutation of the *FLC* 3′ genomic region hybridizing to the small RNAs led to *FLC* misexpression and delayed flowering, suggesting that this pathway is a functionally important component of the endogenous pathways that suppress *FLC* expression.

The simplest model to account for these observations is that the small RNAs are derived from the *FLC* 3′ region, perhaps through the activity of NRPD1a, directly or indirectly generating an antisense transcript that is a target for DCL3. It is possible that the RNAi machinery generates many different small RNAs corresponding to this region. For some reason, the 30- and 24-nt small RNA may be the most stable and so accumulate to detectable levels. The small RNAs would then be involved in recruitment of chromatin complexes to specific *FLC* sequences that methylate histones at specific nucleosome(s) located just downstream from the major poly(A) site, leading to reduced expression of *FLC*. Two mechanisms seem

plausible to account for how the small RNA leads to reduction in *FLC* expression. The first one would involve a reduced level of transcription leading to less *FLC* mRNA being made. The other would involve inefficient polyadenylation of *FLC* transcripts. For example, localized heterochromatin at *FLC* 3′ could negatively affect proper polyadenylation so that aberrant transcripts are produced and processed by a DCL3-dependent mechanism, reinforcing silencing at the *FLC* 3′ end. This possibility seems attractive given the coincidence of the small RNAs and localized chromatin changes to just a few nucleotides downstream from the major poly(A) site. A connection with polyadenylation opened up the possibility of involvement of the autonomous floral pathway. In this pathway, FCA, an RNA-binding protein, interacts with FY, a homolog of a yeast RNA 3′ processing factor Pfs2p (29, 30). Their function in RNA processing has been analyzed through their effects on the regulation of the *FCA* transcript that accumulates in different forms. *fca* or *fy* mutations increase use of a distal poly(A) site, whereas overexpression of FCA leads to exclusive use of a proximal site within *FCA* intron 3, resulting in an FY-dependent negative feedback regulation of *FCA* (29, 31). These data suggest that FCA/FY thus regulate poly(A) site choice perhaps by recruiting specific transcripts or stabilizing weak poly(A) site interactions. Because the *fca-9* mutant did not lack *FLC* 3′ small RNA molecules, these different connections to polyadenylation maybe coincidental with FCA not playing a significant role in the small RNA-silencing mechanism described here. Alternatively, *FCA* may function downstream from the *DCL3*-generated small RNA, or the function of FCA with regard to *FLC* 3′ small RNA may be redundant, being shared with some other component of the autonomous pathway.

The functional significance of the enrichment of *FLC* 3′ small RNA in siliques compared with seedlings is not clear. However, empirical observations by a number of groups have shown that small RNAs are generally more abundant in reproductive tissues (5). Thus, it could represent a general property of this type of regulation, or it could be specific to *FLC*, defining a pathway that regulates *FLC* levels either in reproductive tissues or embryos. We still know comparatively little about the relative contributions of the different pathways regulating *FLC* over the plant life cycle. An assumption that is often made is that it is expression in the young seedling that determines the timing of flowering. However, many of the components of the autonomous and FRIGIDA pathways regulating *FLC* are expressed, often most strongly, in embryos (C.D., unpublished observations), and establishment of high *FLC* levels in embryos has been postulated to be important to avoid precocious flowering (31).

This work may also provide some insight into the biological function of the widespread antisense transcription taking place in eukaryotic genomes (12). It is well established that the vast majority of RNA transcripts are retained in the nucleus. Many of the antisense transcripts overlapping genes may be directed into RNAi pathways to produce small RNA molecules that in turn could help target chromatin complexes to chromatin containing complementary DNA sequences thus mediating expression changes.

Materials and Methods

Plant Materials and Growth Conditions. Plants were grown in a controlled environment room with a 16-h photoperiod composed of 10 h from 400-W Wotan metal halide lamps and 100-W tungsten halide lamps and a 6-h extension of exclusively tungsten halide lamps at 20°C (Sanyo Gallenkamp, Loughborough, U.K.) after being stratified for 2 days at 4°C in an 8-h photoperiod. Young seedlings were transferred to trays with 2- × 2-cm cells. Flowering time was measured by counting total leaf number, which was scored as the number of rosette leaves plus cauline leaves. Plants were also grown on Petri dishes containing GM medium (1× Murashige and Skoog salts/1% glucose/0.5 mg/liter pyridoxine/0.5 mg/liter nicotinic acid, 0.5 mg/liter thymidine/100 mg/liter inositol/0.5 g/liter Mes/0.8% agar, pH 5.7).

flc_utr3, *flc_utr4*, and *fcl_utr5* were obtained from Nottingham *Arabidopsis* Stock Centre (Nottingham, U.K.) and corresponded to Salk T-DNA insertion mutants: SALK_140021, SALK_131491, and SALK_125277.52.80.X, respectively. *dcl2-1*, *dcl3-1*, and *rdr2-1* were provided by J. Carrington (2). *dcl3-2* T-DNA insertion line (CS849593) was obtained from *Arabidopsis* Biological Resource Center (Columbus, OH). *dcl2-1*, *dcl3-1*, *dcl4-1* triple mutant was generated by F. Liu. *nrpd1a-3* and *nrpd1a-4* were provided by Alan Herr and David Baulcombe (Sainsbury Laboratory, Norwich, U.K.). *fld-3* was provided by R. Amasino (32). *fca-9* was provided by Chang-Hsien Yang (National Chung Hsing University, Taiwan).

Expression Analysis. A hot phenol RNA extraction was undertaken as described (33). Blotted membranes were probed with a region of *FLC* corresponding to bases 297–705 of *FLC* cDNA (GenBank accession no. AF116527), a *β-TUBULIN* probe specific for At1g20010. Strand-specific RT-PCR was performed with 0.5 μg of RNA extracted with RNeasy Plant mini kit (Qiagen, Valencia, CA) with an on-column DNase digestion step (Qiagen), followed by Turbo DNase (Ambion, Austin, TX) treatment. RT-PCR was performed with a One Step RT-PCR kit (Qiagen) plus reverse transcription primer, followed by the addition of a second primer for the PCR step. Primers used are shown in SI Table 1.

ChIP Protocol. ChIP assays were performed as described previously (34) with minor modifications. Chromatin preparations from *Arabidopsis* Col-0 siliques were immunoprecipitated with anti-H3K9me2 antibody (rabbit 4677 from Thomas Jenuwein, IMP Research Vienna, Austria) and magnetic Dynabeads protein A (Invitrogen, Carlsbad, CA). ChIP DNA was analyzed by semiquantitative PCR as described (34). Ta3 primers were obtained from sources described in ref. 35. Each ChIP was repeated twice.

Small RNA Analysis. RNA was extracted from plant leaf or inflorescence tissues by using TRIzol reagent (Invitrogen) followed by PEG precipitation. Gel electrophoresis and blot hybridization were undertaken as described (36). An RNA Decade marker (Ambion) was used for sizing small RNA.

We thank Thomas Jenuwein for the H3K9me2 antibody and Judith Irwin for critically reading the manuscript. S.S. and A.J. were supported by Polish Ministry of Science and Higher Education Grants PBZ 089/PO6/2003 and PO4A 03928. S.S.'s time at the John Innes Center was supported by British Council Grants YSP 2004 and 2006. P.C. and F.L. were supported by Biotechnology and Biological Sciences Research Council G 208/G17507.

1. Matzke MA, Birchler JA (2005) *Nat Rev Genet* 6:24–35.
2. Xie Z, Johansen LK, Gustafson AM, Kasschau KD, Lellis AD, Zilberman D, Jacobsen SE, Carrington JC (2004) *PLoS Biol* 2:e104.
3. Zilberman D, Cao X, Jacobsen SE (2003) *Science* 299:716–719.
4. Boutet S, Vazquez F, Liu J, Beclin C, Fagard M, Gratias A, Morel JB, Crete P, Chen X, Vaucheret H (2003) *Curr Biol* 13:843–848.
5. Herr AJ, Jensen MB, Dalmay T, Baulcombe DC (2005) *Science* 308:118–120.
6. Onodera Y, Haag JR, Ream T, Nunes PC, Pontes O, Pikaard CS (2005) *Cell* 120:613–622.
7. Kanno T, Huettel B, Mette MF, Aufsatz W, Jaligot E, Daxinger L, Kreil DP, Matzke M, Matzke AJM (2005) *Nat Genet* 37:761–765.
8. Pontier D, Yahubyan G, Vega D, Bulski A, Saez-Vasquez J, Hakimi MA, Lerbs-Mache S, Colot V, Lagrange T (2005) *Genes Dev* 19:2030–2040.
9. Lu C, Tej SS, Luo S, Haudenschild CD, Meyers BC, Green PJ (2005) *Science* 309:1567–1569.
10. Qi Y, He X, Wang XJ, Kohany O, Jurka J, Hannon GJ (2006) *Nature* 443:1008–1012.
11. Haussecker D, Proudfoot NJ (2005) *Mol Cell Biol* 25:9724–9733.

12. Yamada K, Lim J, Dale JM, Chen H, Shinn P, Palm CJ, Southwick AM, Wu HC, Kim C, Nguyen M, *et al.* (2003) *Science* 302:842–846.
13. Lee S, Bao J, Zhou G, Shapiro J, Xu J, Shi RZ, Lu X, Clark T, Johnson D, Kim YC, *et al.* (2005) *RNA* 11:939–946.
14. Borsani O, Zhu J, Verslues PE, Sunkar R, Zhu JK (2005) *Cell* 123:1279–1291.
15. Katiyar-Agarwal S, Morgan R, Dahlbeck D, Borsani O, Villegas A, Jr, Zhu JK, Staskawicz BJ, Jin H (2006) *Proc Natl Acad Sci USA* 103:18002–18007.
16. Sheldon CC, Burn JE, Perez PP, Metzger J, Edwards JA, Peacock WJ, Dennis ES (1999) *Plant Cell* 11:445–458.
17. Michaels SD, Amasino RM (1999) *Plant Cell* 11:949–956.
18. Gendall AR, Levy YY, Wilson A, Dean C (2001) *Cell* 107:525–535.
19. Levy YY, Mesnage S, Mylne JS, Gendall AR, Dean C (2002) *Science* 297:243–246.
20. Sung S, Amasino RM (2004) *Nature* 427:159–164.
21. Bastow R, Mylne JS, Lister C, Lippman Z, Martienssen RA, Dean C (2004) *Nature* 427:164–167.
22. Mylne JS, Barrett L, Tessadori F, Mesnage S, Johnson L, Bernatavichute YV, Jacobsen SE, Fransz P, Dean C (2006) *Proc Natl Acad Sci USA* 103:5012–5017.
23. Sung S, He Y, Eshoo TW, Tamada Y, Johnson L, Nakahigashi K, Goto K, Jacobsen SE, Amasino RM (2006) *Nat Genet* 38:706–710.
24. Baurle I, Dean C (2006) *Cell* 125:655–664.
25. Gustafson AM, Allen E, Givan S, Smith D, Carrington JC, Kasschau KD (2005) *Nucleic Acids Res* 33:D637–D640.
26. Yang Z, Ebright YW, Yu B, Chen X (2006) *Nucleic Acids Res* 34:667–675.
27. Zilberman D, Cao X, Johansen LK, Xie Z, Carrington JC, Jacobsen SE (2004) *Curr Biol* 14:1214–1220.
28. Quesada V, Dean C, Simpson GG (2005) *Int J Dev Biol* 49:773–780.
29. Simpson GG, Dijkwel PP, Quesada V, Henderson I, Dean C (2003) *Cell* 113:777–787.
30. Henderson IR, Liu F, Drea S, Simpson GG, Dean C (2005) *Development (Cambridge, UK)* 132:3597–3607.
31. Quesada V, Macknight R, Dean C, Simpson GG (2003) *EMBO J* 22:3142–3152.
32. He Y, Michaels S, Amasino R (2003) *Science* 302:1751–1754.
33. Etheridge N, Trusov Y, Verbelen JP, Botella JR (1999) *Plant Mol Biol* 39:1113–1126.
34. Gendrel A-V, Lippman Z, Yordan C, Colot V, Martienssen RA (2002) *Science* 297:1871–1873.
35. Johnson LM, Cao X, Jacobsen SE (2002) *Curr Biol* 12:1360–1367.
36. Allen E, Xie Z, Gustafson AM, Sung GH, Spatafora JW, Carrington JC (2004) *Nat Genet* 36:1282–1290.